Available online at www.sciencedirect.com
SCIENCE DIRECT
ELSEVIER
Synthetic Metals 153 (2005) 409–412
SYNTHETIC METALS
www.elsevier.com/locate/synmet

Scanning Tunneling Spectroscopy on κ-(BEDT-TTF)$_2$Cu[N(CN)$_2$]Br

K. Ichimura*, S. Higashi, K. Nomura, A. Kawamoto

Division of Physics, Hokkaido University, Sapporo 060-0810, Japan

Abstract

We report the electron tunneling spectroscopy on partially deuterated κ-(BEDT-TTF-d[3,3])$_2$Cu[N(CN)$_2$]Br using a low temperature STM. In the superconducting state, tunneling spectra show the energy gap structure clearly; the conductance around the zero bias voltage is well reduced. V-shaped tunneling conductance curve inside the gap edge suggests the gap anisotropy. The linear dependence on the energy near zero bias is explained by the *d*-wave pairing with line nodes. By fitting to the *d*-wave gap model, we obtain the gap parameter as Δ=1.4-3.3 meV. Correspondingly, $2\Delta/kT_c$ is estimated as 2.7-6.4. The value is almost the same as that in κ-(BEDT-TTF)$_2$Cu(NCS)$_2$, d[0,0] and d[2,2] salts. The zero bias anomaly, which is an evidence for nodes of the superconducting gap, was found. The *d*-wave symmetry is strongly supported.

Keywords: atomic force microscopy, scanning tunneling microscopy, single-crystal surfaces, superconducting phase transitions, organic superconductors

1. Introduction

The quasi-two dimensional electronic band with strongly correlated electrons plays an important role in BEDT-TTF salts, similarly to high-T_c oxides. It is recognized that the superconducting phase adjoins the antiferromagnetic phase [1] in contrast to high-T_c cuprates in which these phases are separated by the anomalous metallic phase [2]. A lot of attentions have been given to which mechanism brings about the superconductivity in the neighbor of the Mott insulating phase. The *d*-wave pairing has been discussed theoretically [3-5]. In the phase diagram with respect to the effective correlation, κ-(BEDT-TTF)$_2$Cu[N(CN)$_2$]Br is located near the boundary between the superconducting and antiferromagnetic phases. Protonated d[0,0] salt undergoes the superconductivity while fully deuterated d[4,4] salt is just on the boundary. Kawamoto *et al.* [6] revealed that the effective correlation can be controlled finely near the Mott boundary by partial deuteration of BEDT-TTF molecules.

In investigating the superconducting state, the electron tunneling is useful since the electronic density of states can be obtained directly with high energy resolution [7]. The tunneling spectroscopy using STM, *i.e.* scanning tunneling spectroscopy (STS), especially has an advantage because of non-contacting tip configuration. The local electronic density of states can be studied directly in superconductors. The microscopic structure of vortices in 2*H*-NbSe$_2$ [8] and the quasi-particle scattering resonance at impurity sites in $Bi_2Sr_2CaCu_2O_8$ [9] were observed clearly with atomic resolution.

STS study on κ-(BEDT-TTF)$_2$Cu(NCS)$_2$ suggested that the superconducting gap is highly anisotropic [10]. We revealed the *d*-wave paring symmetry in κ-(BEDT-TTF)$_2$Cu(NCS)$_2$ by STS on lateral surfaces [11]. In that work, we determined the nodal direction of the gap as π/4 from k_b and k_c axis. Our next interest is how the paring symmetry and the gap parameter depend on the effective correlation. We have already reported tunneling spectra obtained by STS on protonated d[0,0] and partially deuterated d[2,2] κ-(BEDT-TTF)$_2$Cu[N(CN)$_2$]Br [12, 13]. We found that $2\Delta/kT_c$ increases with increasing the effective correlation strength. In this article, we present STS results on κ-(BEDT-TTF-d[3,3])$_2$Cu[N(CN)$_2$]Br, which is located closer to the Mott boundary.

The bound state at the gap node is an important feature which characterizes anisotropic superconductors, since it reflects the phase of the order parameter. Such a bound state is observed as the zero bias conductance peak (ZBCP) in tunneling spectra [14]. The ZBCP is popular in high-T_c cuprates [15-17] of which pairing symmetry is the *d*-wave. Although the *d*-wave pairing has been suggested in BEDT-TTF superconductors, the ZBCP has not been observed yet. In this paper, we present not only the superconducting gap but also the first observation of the ZBCP in organic superconductors.

* Corresponding author. Tel: +81-11-706-4431; Fax: +81-11-706-4926; E-mail: ichimura@sci.hokudai.ac.jp

doi:10.1016/j.synthmet.2005.07.318

2. Experimental

Single crystals with hexagonal plate were grown by standard electro-chemical method. Typical dimension of single crystals is about 1×1×0.1 mm^3. Samples were cooled slowly around 80 K with rate of about −0.05 K/min. The superconducting transition temperature was determined as T_c=12.0 K from magnetic transition with applying the magnetic field of 10 Gauss by SQUID magnetometer. The fraction of superconducting phase is estimated as about 10 % from the Meissner volume fraction. As grown surface of the *a-c* plane was investigated by a low temperature STM. The tunneling current flows normal to the conducting layer in this configuration. Mechanically sharpened Pt-Ir wire was used as an STM tip. The tunneling differential conductance was directly obtained by the lock-in detection, in which 1 kHz ac modulation with amplitude of 0.1 mV was superposed in the ramped bias voltage with period of 15 s.

3. Results and Discussion

The superconducting and antiferromagnetic insulating phases coexist in κ-(BEDT-TTF-d[3,3])$_2$Cu[N(CN)$_2$]Br. Our slow cooling rate of -0.05 K/min at 80 K increases the fraction of the superconducting phase. When we could probe the superconducting region by STM, tunneling spectra show the energy gap structure clearly. Figure 1 shows the tunneling differential conductance curve at various samples for κ-(BEDT-TTF-d[3,3])$_2$Cu[N(CN)$_2$]Br. Curves are normalized by the conductance at 10 mV. In all curves, the differential conductance around the zero bias voltage is well reduced compared with the normal conductance. Details of the curve at high energy region differ from sample to sample. Some spectra show peak at the gap edge while other spectra show shoulder. The magnitude of the gap varies depending on sample. However, we would like to emphasize that the functional form at low energy region, which reflects the symmetry of the pair wave function, is identical.

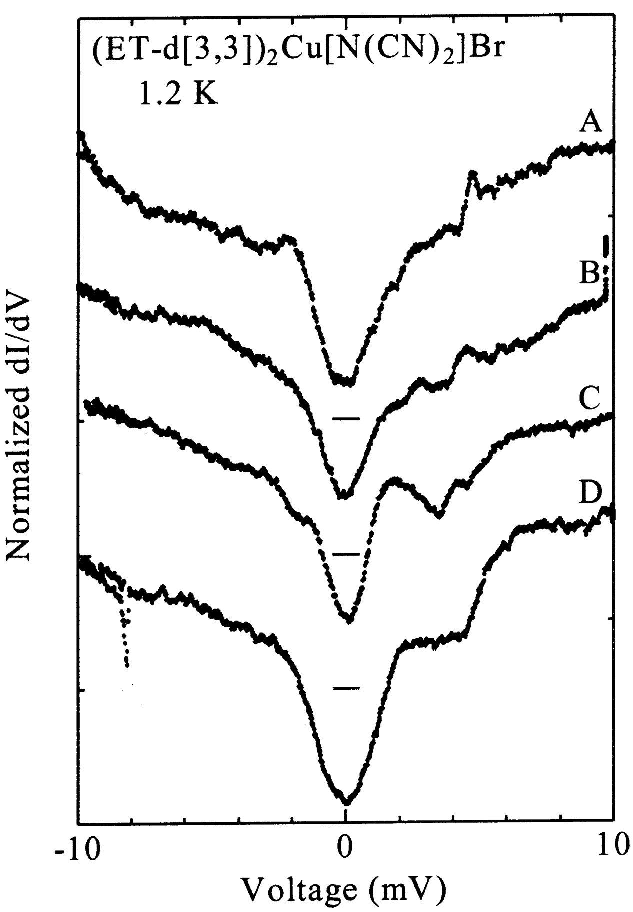

Fig. 1. Normalized tunneling differential conductance in the superconducting state for four different samples of κ-(BEDT-TTF-d[3,3])$_2$Cu[N(CN)$_2$]Br. The zero conductance line of each curve, which is represented by the horizontal bar, is shifted by one division for clarity.

Figure 2 shows a typical tunneling conductance curve. At first, we examine the *s*-wave symmetry which brings about the isotropic gap. We try to fit the spectra by the Dynes eq. [18] described as,

$$\frac{N_S(E)}{N_N(0)} = \mathrm{Re}\left[\frac{E - i\Gamma}{\sqrt{(E - i\Gamma)^2 - \Delta^2}}\right] \tag{1}$$

where N_N and N_S are the electronic density of states in the normal and superconducting state, respectively. The quasi-particle lifetime broadening is taken into account by the parameter Γ. It is well known that tunneling spectra of

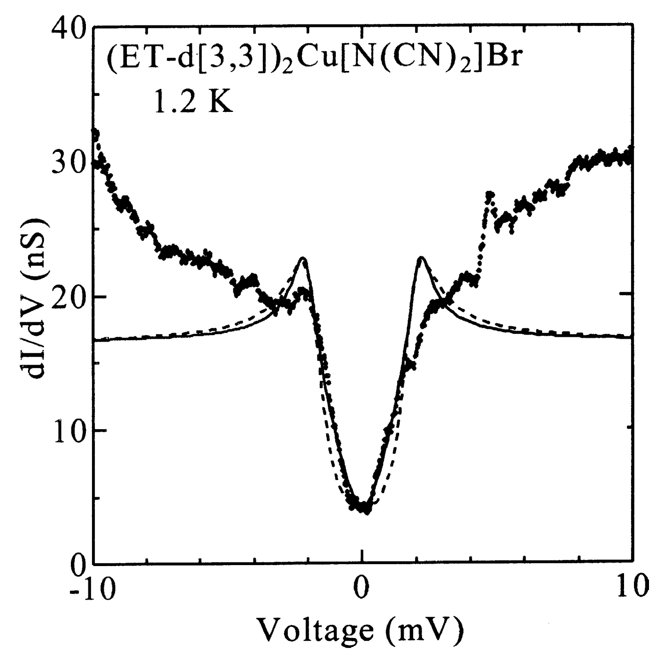

Fig. 2. Typical tunneling spectra. The broken and solid lines represent calculated conductance curves based on the *s*-wave and *d*-wave symmetry, respectively.

conventional s-wave superconductors are fitted by the Dynes eq. For the s-wave case, the remained conductance around zero bias voltage is explained by the lifetime broadening and the thermal smearing. The broken line in Fig. 2 represents the Dynes eq. with the gap parameter Δ=1.8 meV and the lifetime broadening parameter Γ=0.36 meV. As shown in Fig. 2, the spectra cannot be fitted by the Dynes eq. The tunneling conductance at low energy is larger than the calculated Dynes eq. The finite conductance inside the gap is brought about not only by the lifetime broadening but also the gap anisotropy.

Next we examine the d-wave symmetry with line nodes. We use a trial function with the d-wave symmetry as the simplest form described as,

$$\Delta(\boldsymbol{k}) = \Delta\cos(2\phi)\,. \qquad (2)$$

We assume that the electronic band dispersion is isotropic in the calculation [19]. The solid line in Fig. 2 represents the calculated conductance curve based on the d-wave. In the fitting, the life time broadening is taken into account by introducing the parameter Γ. Values are obtained as Δ=2.1 meV and Γ=0.21 meV by the fitting. The linear dependence on the energy inside the gap is well explained by the d-wave symmetry. The remained conductance at zero voltage is reproduced by a small lifetime broadening Γ. The d-wave symmetry is suggested for the pair wave function similarly to other BEDT-TTF superconductors. For κ-(BEDT-TTF-d[3,3])$_2$Cu[N(CN)$_2$]Br, the gap parameter is obtained by as Δ=1.4-3.3 meV by the above fitting. Correspondingly, the reduced gap is obtained as $2\Delta/kT_c$=2.7-6.4. The scatter in value is due to sample dependence.

Gap values for d[0,0] [12], d[2,2] [13] and d[3,3] salts are listed in Table 1. These values are almost consistent with that for κ-(BEDT-TTF)$_2$Cu(NCS)$_2$ [20]. The effective correlation strength U/W, where U is the on-site Coulomb interaction and W is the band width, becomes large by the deuteration. In comparing between d[0,0] and d[2,2], the reduced gap increases with increasing U/W. However, the reduced gap for d[3,3] salt is smaller than that for both d[0,0] and d[2,2] salt. We find that $2\Delta/kT_c$ does not increase monotonically close to the Mott boundary.

It is noteworthy that the value of $2\Delta/kT_c$ for κ-(BEDT-TTF-d[n,n])$_2$Cu[N(CN)$_2$]Br and κ-(BEDT-TTF)$_2$Cu(NCS)$_2$ is larger than the prediction of 4.35, which is according to the mean field theory for d-wave superconductors [21]. It suggests the strong coupling superconductivity in BEDT-TTF salts.

We would like to mention about the remained conductance at zero bias voltage. For κ-(BEDT-TTF-d[n,n])$_2$Cu[N(CN)$_2$]Br, the normalized conductance at zero bias voltage, which is about 10-20% of the conductance in the normal state, is larger than that for κ-(BEDT-TTF)$_2$Cu(NCS)$_2$. The lifetime broadening parameter Γ, which are used in the fit by the d-wave, for κ-(BEDT-TTF-d[n,n])$_2$Cu[N(CN)$_2$]Br is about twice as large as that for κ-(BEDT-TTF)$_2$Cu(NCS)$_2$, in which Γ is less than 0.1 meV [20]. We think that there is some disorders in κ-(BEDT-TTF-d[n,n])$_2$Cu[N(CN)$_2$]Br.

It should be noted that anomalous enhancement of conductance around zero bias is observed occasionally. Figure 3 shows the tunneling spectra with such anomaly. Curves for two different samples are shown. The tunneling conductance at zero bias voltage increases divergently in contrast to the case of the superconducting gap. We think that this sharp peak corresponds to the zero bias conductance peak (ZBCP) unique to d-wave superconductors. The ZBCP has already been found in high-T_c cuprates $Bi_2Sr_2CaCu_2O_8$ [15], $La_{2-x}Sr_xCuO_4$ [16] and $YBa_2Cu_3O_7$ [17]. The present result is the first observation of the ZBCP in BEDT-TTF superconductors. The ZBCP is caused by the zero energy state, which is the bound state formed around gap nodes where the sign of the order parameter changes [14]. The essential point of the origin of the bound state is that electron and hole like quasi-particle, which are due from injected electrons into

Table 1.
Gap parameter Δ and corresponding $2\Delta/kT_c$ for κ-(BEDT-TTF-d[n,n])$_2$Cu[N(CN)$_2$]Br.

	Δ (meV)	$2\Delta/kT_c$
d[0,0]	2.1-3.9	4.3-7.9
d[2,2]	3.0-4.8	5.8-9.3
d[3,3]	1.4-3.3	2.7-6.4

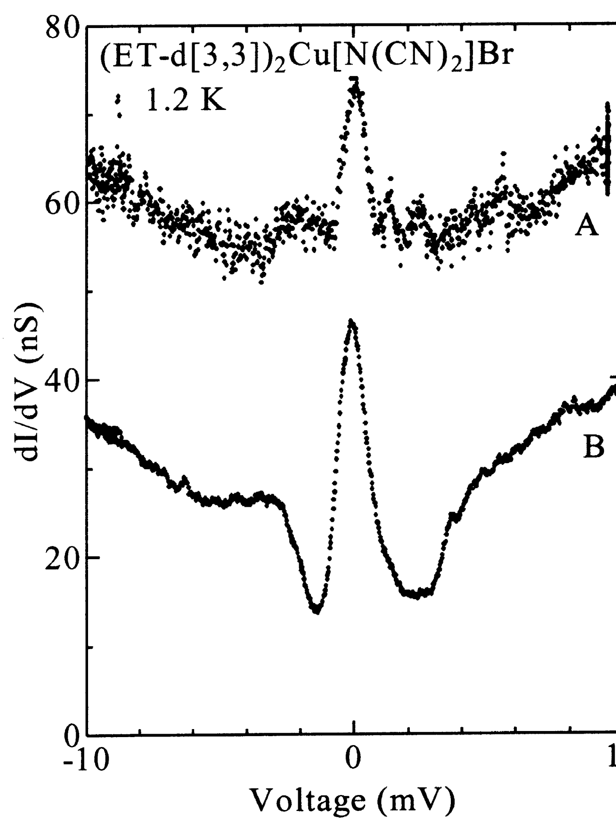

Fig. 3. Tunneling spectra with the zero bias anomaly. Curves for two different samples are shown. The zero conductance line of each curve is shifted by 20 nS for clarity.

superconductor, feel opposite sign of pair potentials. It should be noted that the ZBCP is the phase sensitive phenomenon. Therefore, the ZBCP is thought to be a direct evidence for nodes of the superconducting gap. The ZBCP in our tunneling spectra strongly supports the *d*-wave pairing symmetry in BEDT-TTF superconductors.

Normally, one can hardly observe the ZBCP in the present tunneling configuration, in which electrons tunnel perpendicular to the conducting plane. The in-plane anisotropy would be averaged out. It is essential that electrons with wave number around the gap nodes contribute selectively to the tunneling in observing the ZBCP. We think that micro steps or any disorder of the surface enabled us to observe the ZBCP. The in-plane component of the wave number can be resolved in the tunneling from step edges. Actually, the ZBCP was sometimes observed at the *c*-direction tunneling in high-T_c cuprates [14]. In addition, domain boundaries between the superconducting and insulating phases might help the tunneling electron to flow along the conducting plane in κ-(BEDT-TTF-d[3,3])$_2$Cu[N(CN)$_2$]Br.

We could not find the ZBCP in the tunneling at lateral surfaces for κ-(BEDT-TTF)$_2$Cu(NCS)$_2$ [11] in contrast to the present results on κ-(BEDT-TTF-d[3,3])$_2$Cu[N(CN)$_2$]Br. One possible reason is that we could not probe just node direction in the previous work on lateral surfaces. The ZBCP is sensitive to the direction of the wave vector of tunneling electrons. The directional dependent tunneling is discussed according to WKB approximation [22]. The angle, in which the tunneling probability decays by a factor of *e*, of our STS configuration on BEDT-TTF salts is estimated as 13 degrees [11]. The angle window is narrower than that for $Bi_2Sr_2CaCu_2O_8$ of 22 degrees [15]. A little deviation from the node direction makes difficult to observe the ZBCP.

Another possible reason is difference in geometry of the Fermi surface. For κ-(BEDT-TTF)$_2$Cu(NCS)$_2$, the Fermi surface is separated at the zone boundary due to the asymmetrical arrangement of anions [23]. As a result, the gap opens at the direction around $\pi/4$ from k_b and k_c axis. It suggests that there is no metallic state around gap nodes Therefore, the possibility that no ZBCP is intrinsically found should be pointed out for κ-(BEDT-TTF)$_2$Cu(NCS)$_2$. On the other hand, there is no gap on the Fermi surface for κ-(BEDT-TTF)$_2$Cu[N(CN)$_2$]Br [24]. From this point of view, κ-(BEDT-TTF)$_2$Cu[N(CN)$_2$]Br is suitable to study the ZBCP.

We cannot know the nodal direction in κ-(BEDT-TTF-d[3,3])$_2$Cu[N(CN)$_2$]Br by the present tunneling configuration since we could not succeed the morphologic survey of the microscopic step edge. Recent theoretical study [25] predicted that which order parameter $d_{x^2-y^2}$ or d_{xy}-wave is favorable depending on strength of the dimerization. We are interested in the phase of the order parameter in κ-(BEDT-TTF)$_2$Cu[N(CN)$_2$]Br in comparison with that in κ-(BEDT-TTF)$_2$Cu(NCS)$_2$, in which the $d_{x^2-y^2}$ wave symmetry is suggested. STS at lateral surfaces in κ-(BEDT-TTF)$_2$Cu[N(CN)$_2$]Br is our future study to determine the direction of nodes. Tanuma *et al.* [26] predicted that ZBCP in BEDT-TTF salts splits into two peaks due to the multiband effect. They also proposed that the peak splitting is the probe to distinguish the pairing symmetry. Details of ZBCP in BEDT-TTF salt should be investigated.

4. Conclusion

The superconducting phase of partially deuterated κ-(BEDT-TTF-d[n,n])$_2$Cu[N(CN)$_2$]Br was investigated by STS. Conductance curves are explained by the *d*-wave symmetry. The gap parameter is obtained for d[0,0], d[2,2] and d[3,3] salts. $2\Delta/kT_c$ for d[2,2] salt is larger than that for d[0,0] salt as the effective correlation increases. However, the reduced gap for d[3,3] salt is smaller than that both for d[0,0] and d[2,2] salt. Larger value of $2\Delta/kT_c$ than that of the mean field theory for *d*-wave superconductors suggests strong coupling. The ZBCP which is a direct evidence for gap nodes was found. The *d*-wave pairing symmetry is strongly supported in BEDT-TTF superconductors.

References

[1] K. Kanoda, Hyperfine Interact. 104 (1997) 235.
[2] B. Batllog, V. J. Emery, Nature 382 (1996) 20.
[3] R. Arita, K. Kuroki, H. Aoki, J. Phys. Soc. Jpn. 69 (2000) 1181.
[4] B. J. Powell, R. H. McKenzie, Phys. Rev. B 69 (2004) 024519.
[5] J. X. Li, Phys. Rev. Lett. 91 (2003) 037002.
[6] A. Kawamoto, H. Taniguchi, K. Kanoda, J. Am. Chem. Soc. 120 (1998) 10984.
[7] I. Gieaver, Phys. Rev. Lett. 5 (1960) 147.
[8] H. F. Hess, R. B. Robinson, R. C. Dynes, J. M. Valles, Jr., J. V. Waszczak, Phys. Rev. Lett. 62 (1989) 214.
[9] S. H. Pan, E. W. Hudson, K. M. Lang, H. Eisaki, S. Uchida, J. C. Davis, Nature, 403 (2000) 746.
[10] K. Ichimura, T. Arai, K. Nomura, S. Takasaki, J. Yamada, S. Nakatsuji, H. Anzai, Synth. Metals, 85 (1997) 1543.
[11] T. Arai, K. Ichimura, K. Nomura, S. Takasaki, J. Yamada, S. Nakatsuji, H. Anzai, Phys. Rev. B 63 (2001) 104518.
[12] K. Ichimura, K. Suzuki, K. Nomura, A. Kawamoto, Synth. Metals, 133-134 (2003) 213.
[13] K. Ichimura, K. Suzuki, K. Nomura, A. Kawamoto, Synth. Metals, 137 (2003) 1229.
[14] S. Kashiwaya, Y. Tanaka, Rep. Prog. Phys. 63 (2000) 1641.
[15] K. Suzuki, K. Ichimura, K. Nomura, S. Takekawa, J. Phys.: Condens. Matter 11 (1999) 3133.
[16] S. Tanaka, E. Ueda, M. Sato, K. Tamasaku, S. Uchida, J. Phys. Soc. Jpn. 64 (1995) 1476.
[17] S. Kashiwaya, Y. Tanaka, H. Takashima, Y. Koyanagi, K. Kajimura, Rev. B 51 (1995) 1350.
[18] R. C. Dynes, V. Narayanamurti, J. P. Garno, Phys. Rev. Lett. 41 (1978) 1509.
[19] K. Ichimura, K. Nomura, J. Phys. Soc. Jpn. 62 (1993) 3661.
[20] T. Arai, K. Ichimura, K. Nomura, S. Takasaki, J. Yamada, S. Nakatsuji, H. Anzai, Solid State Commun. 116 (2000) 679.
[21] F. J. Ohkawa, J. Phys. Soc. Jpn. 56 (1987) 2267.
[22] E. L. Wolf, Principles of Electron Tunneling Spectroscopy, Oxford University Press, New York (1989).
[23] K. Oshima, T. Mori, H. Inokuchi, H. Urayama, H. Yamochi, G. Saito, Phys. Rev. B 38 (1988) 938.
[24] U. Geiser, A. J. Schultz, H. H. Wang, D. M. Watkins, D. L. Stupka, J. M. Williams, J. E. Shirber, D. L. Overmyer, D. Jung, J. J. Nova, M. H. Whangbo, Physica. C 174 (1991) 475.
[25] K. Kuroki, K. Kimura, R. Arita, Y. Tanaka, Y. Matsuda, Phys. Rev. B 65 (2002) 10516.
[26] Y. Tanuma, K. Kuroki, Y. Tanaka, S. Kashiwaya, Phys. Rev. B 68 (2003) 214513.